

Fractal Dimensional Classification of Aerosol Particles by Computer-Controlled Scanning Electron Microscopy

Volodymyr V. Kindratenko, Piet J. M. Van Espen,* Boris A. Trejger, and René E. Van Grieken

Department of Chemistry, University of Antwerp (UIA), Universiteitsplein 1, B-2610 Antwerpen-Wilrijk, Belgium

A method for the classification of individual aerosol particles into one of two main groups, namely, fly ash and soil dust, is presented. It is based on the calculation of the fractal dimensions of the images of the particles obtained with the computer-controlled scanning electron microscopy. The risk of an improper determination of the fractal dimension is pointed out. It is shown that spherically shaped particles that normally compose the majority of the fly ash particles do not possess fractality. The rarely met fly ash particles with very irregular shape possess two types of the fractal dimensions, namely, textural and structural. On the other hand, it is found that the soil dust particles have only a textural fractal dimension. The obtained results allow the unequivocal identification of the particle source, which is especially important when the chemical compositions of the particles are nearly the same.

Introduction

Analysis of individual aerosol particles can yield very important environmental information, the relevance of which cannot be overestimated. However, the identification and apportionment of the sources of the particles are often complicated because particles originating from different sources can have similar compositions. The most widespread example is fly ash (usually originating from combustion) and soil dust particles (usually clay minerals), which really have nearly the same compositions. The only parameter that can allow us to differentiate between them is the shape. Therefore, the problem of the characterization of the shape of aerosol particles is very genuine (see e.g., ref 1).

Computer-controlled scanning electron microscopy (CC SEM) in combination with energy-dispersive X-ray microanalysis (EDX) is among the most frequently used methods for obtaining morphological information. Built-in image processing facilities increase substantially its possibilities in various applications where morphological and/or textural information is valuable. The ability to determine also the chemical composition provides a means for automated particle identification and classification. The significance of such an approach has been recognized for a long time (2).

The problem is, however, in revealing and representing the morphological information (textural information, in three-dimensional meaning of these words, is beyond the scope of the present study although without any doubt very essential). An extensive review of the subject can be found, for example, in chapter 9 of a book by Duda and Hart (3). At least, four different methods of particle shape representation are possible. The first and the oldest one is based on different shape factors as described in detail

in ref 4). The main disadvantage is that shape factors are integral characteristics and, as such, may be not sensitive enough to the details of the particle shape. The other three methods are fractal and Fourier analyses and chain coding. Recently, chain coding has been used for shape description while Fourier analysis is a well-established method of shape characterization. The fractal approach to shape characterization, usually considered as a complement to Fourier characterization, certainly is more exotic although there are numerous papers (see, e.g. refs 5 and 6, which deal with the determination of fractal dimension; ref 7, where fractal approach is applied to the description of the shape of airborne particles; and ref 3, a recent publication connected with the evaluation of different methods of calculation of fractal dimensions) and a book by Kaye (9), dedicated to it. However, to our knowledge, questions such as "In which cases is the fractal approach valid?" and "What is the precision of fractal diameter determination?" have never been answered.

The aim of this paper is to examine the applicability of fractals for morphological description of the shapes of individual aerosol particles studied with CC SEM-EDX and to clarify some questions linked with this.

Fractal Description of Particle Shapes: A Brief Overview

Fractal analysis is a very important field of modern mathematics. From the specific point of view of shape characterization of microscopic particles, one can say that the main aim of the fractal approach is to find a 'measure' to distinguish between the curves with different, often very complicated, contours. The main idea is to describe the complexity of the curve through a new parameter, the fractal dimension, so as to fill in the gap between one- and two-dimensional objects (for objects on a plane). The more complex the contour of the curve, the more it covers the plane in a dense manner and the more its fractal dimension will be close to 2. There are numerous textbooks and abundant literature on this subject. Therefore, we will not go into detail and will only briefly describe some facts of the theory of fractals.

The fractal concept is not strictly defined. In spite of this, there is a consensus that fractal objects (among other important features) normally possess a too irregular structure to be described by traditional geometrical or topological approaches. The main characteristic of fractals is their fractal dimension that can be introduced in different ways. As applied to particle shape characterization, it can be established in the following way.

As a consequence of the very irregular structure, the perimeter of the contour depends on the length of the 'stride' or 'yardstick' with which we make measurements. The smaller yardstick can take into account details of the (complicated) shape that are 'invisible' with larger strides. Therefore, the smaller the 'step' L , the larger the perimeter

* E-mail address: Piet.VanEspen@schs.uia.ac.be.

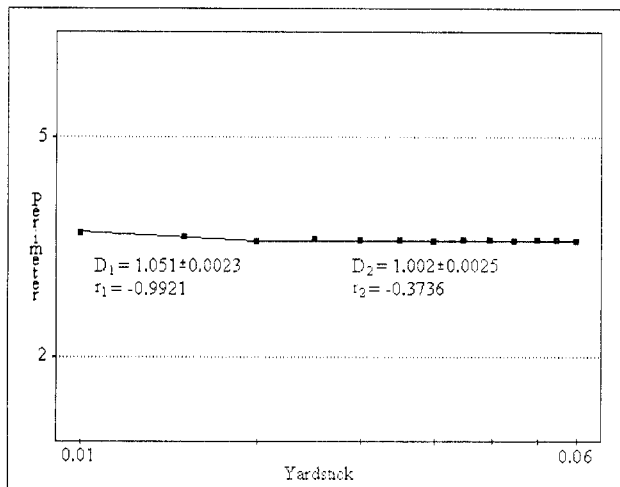


Figure 1. Fractal analysis of the shape of a circle image. Here and in the subsequent Figures 2c, 3c, and 4c the following designations are used: r , the coefficient of correlation for the given regression straight line D , fractal dimension. The yardstick was measured in the fractions of the Feret diameter.

P measured with it. This dependence can be mathematically expressed as

$$P \propto L^\alpha$$

where α is the slope of the log-log plot line. Just this slope is directly connected with fractal dimension D as

$$D = 1 - \alpha$$

From the above explanation, it is obvious that α is negative, so $D > 1$. (We mentioned earlier that for curves on a plane, D should be between 1 and 2.)

An important remark regarding the form of these log-log plots needs to be made. As it was supposed (see ref 10), 'true' fractals should have a single straight line over the whole range of the 'yardsticks' used. Within the framework of the present paper, we can refer to true fractals as objects that have a shape that possesses 'self-similarity'. Self-similarity means that the main 'construction elements' of the contour of the object can be seen for the whole range of the strides. In other words, the higher the magnification with which we observe the object, the more details that can be seen, but the shape of these details is the same for all magnifications. However, in practice, self-similarity has never been observed (11), and usually two straight lines are seen on log-log plots (12). One of them is commonly considered as reflecting the textural fractal dimension, whereas the other one describes the structural one (9). We can refer to them as to microscopic and macroscopic descriptions of the contour shape.

In the majority of references [for instance, a rather recent book (9)], the fractal dimension (especially the textural dimension) is determined using only 5, 4, 3, and even 2(!) points on log-log plot. Often the difference between the two fractal dimensions (between the slopes of the two straight lines) looks insignificant, but no statistical information is provided. The question of the precision of the determination of the fractal dimension was up to now only considered in one publication (13). Moreover, the so-called textural fractals can appear only as a result of the discrete nature of the computer images. Indeed, a circle has definitely no fractality. Figure 1 presents the results of fractal analysis of the digital image of a circle.

One can see that the first three points (corresponding to the first three yardsticks used) exhibit a kind of statistically significant dependence. We observe a false textural fractal. False fractals are called fractal rabbits following the example of Prof. D. Avnir (9). This artificial example of fractal rabbit demonstrates that one should be extremely careful in dealing not only with large strides but also with very small ones.

Types of Shapes of Aerosol Particles

Aerosol particles are characterized by a large variety of sizes and shapes. The shape of the particle is mainly determined by its origin. When we deal with continental aerosols, two main types of aerosol particles, viz., fly ash and soil dust, can be observed. Fly ash originates from various kinds of combustion processes (power plants, metallurgical plants, cars, and other urban sources, etc.), whereas soil dust originates from soil or earth crust dispersion. As a consequence, soil dust particles have a rather pronounced, sometimes very irregular, shape. According to light microscopy studies (14), fly ash particles can be classified into 11 shape classes: (1) amorphous, nonopaque; (2) amorphous, opaque; (3) amorphous, mixed opaque and nonopaque; (4) rounded, vesicular, nonopaque; (5) rounded, vesicular, mixed opaque and nonopaque; (6) angular, lacy, opaque; (7) nonopaque, cenosphere; (8) nonopaque, plerosphere; (9) nonopaque, solid sphere; (10) opaque sphere; (11) nonopaque sphere with crystals. SEM investigations (15) allow us to recognize seven categories of ash particles: (1) unfused detrital minerals (principally quartz); (2) irregular spongy particles derived from partially fused clay minerals; (3) vesicular colorless glass (in the form of irregular particles and cenospheres), derived from viscous melts; (4) solid glass (mostly in the form of spherical particles), derived from fluid melts; (5) dendritic iron oxide particles (mostly spherical); (6) crystalline iron oxide particles (mostly spherical); and (7) unburnt char particles. However, in spite of a such variety of shapes, spherical particles are the most abundant. Depending on the size distribution, their relative abundance sometimes reaches 86% (14).

The composition of the fly ash particles is not so variable as their shape. Among the two main classes, one can mention particles rich in silicon and aluminium oxides (main fraction) and those rich in iron oxide (15). Regarding the soil dust particles, aluminosilicates constitute their main fraction.

Summarizing, we can state that soil dust particles normally have pronounced, irregular shapes, whereas the majority of the fly ash particles have spherical shapes. A limited number of fly ash particles show a very irregular shape. The composition of most of the fly ash and soil dust particles are very similar. In order to study the possibilities of the fractal characterization of the shape, we examined three different types of particles: (1) soil dust; (2) fly ash of spherical shape; and (3) fly ash with irregular shape.

Experimental Section

Sampling. The particles, which were used to test our method, were collected in two different sampling campaigns. The reason that we need two different conditions is to collect fly ash particles of the two different shapes. First of all, we used particles collected in southern Siberia,

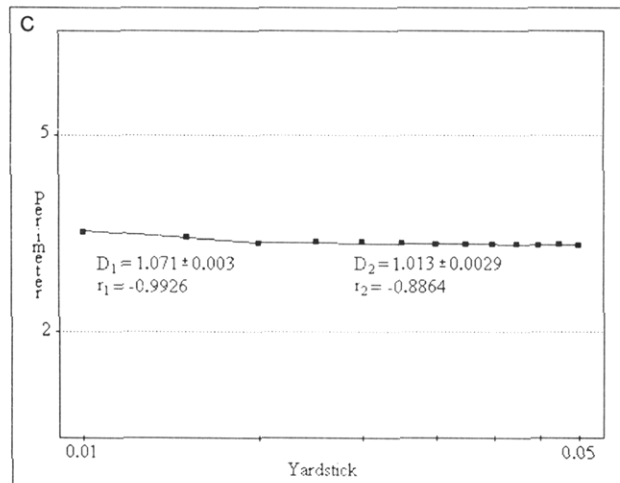
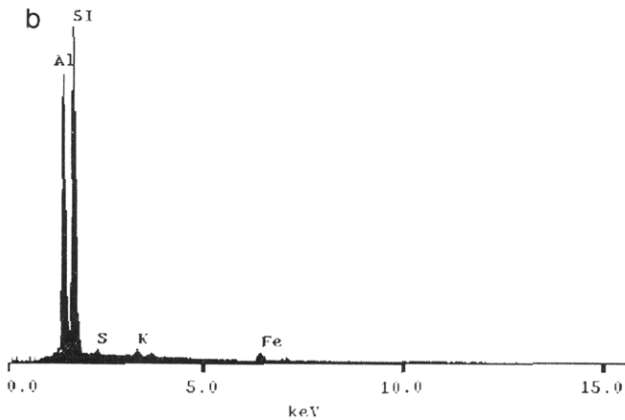
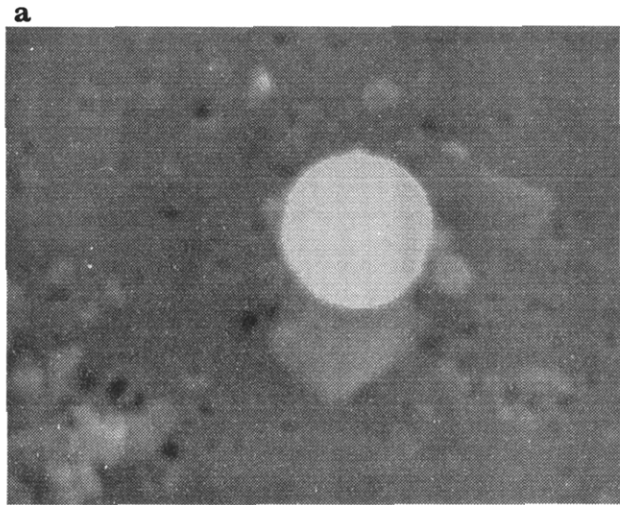


Figure 2. Spherically shaped fly ash particle: (a) SEM micrograph; (b) EDX spectrum; (c) fractal analysis.

Russia, during the winter of 1992. From February 5 to March 4, 1992, aerosol samples were collected three times a day in Karasuk, a relatively small and remote town some 400 km west of Novosibirsk. Our sampling equipment was placed some 8 km west of the town on the shore of a small lake. The sampler was positioned approximately 2 m above the ground. The particles were collected using 47 mm diameter, 0.4- μm pore size Nuclepore polycarbonate membrane filters (aerosol grade). These filters were placed in Plexiglass filter holders with a hat-type cover to protect them from the rain. The vacuum pump was operated at a flow rate of approximately 50 L/min and equipped with a flowmeter. In this case, most of the particles were spherically shaped fly ash particles.

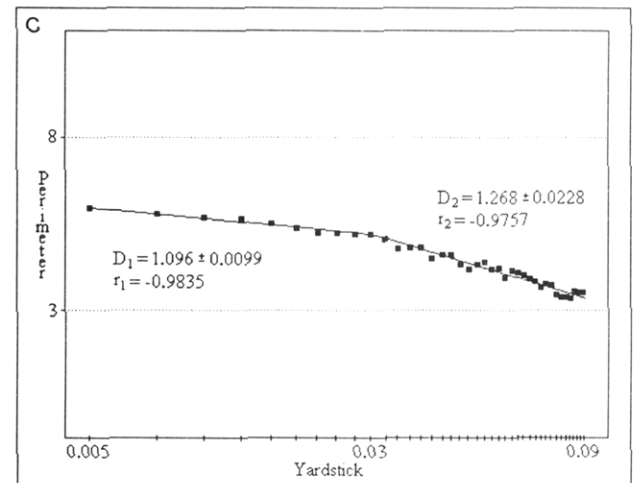
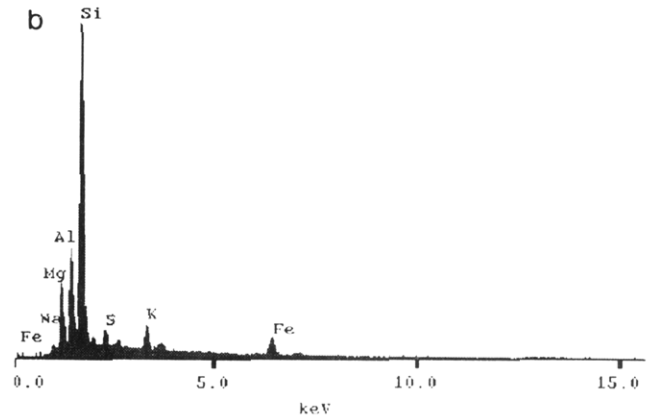


Figure 3. Irregularly shaped fly ash particle: (a) SEM micrograph; (b) EDX spectrum; (c) fractal analysis.

Other aerosols used in our research were collected during a forest fire in the delta of the River Podkamennaya Tunguska in Russia on July 6, 1993. The sampling equipment was lifted above the fire with the help of a helicopter. A small sampler for material dispersed by the fire was loaded with 0.4- μm pore size Nuclepore filters. Aerosols were sampled during numerous flights through the smoke column. In this way, samples with irregularly shaped fly ash particles were acquired.

CC SEM. The measurements were performed on a JEOL JSM-6300 electron microscope using an electron energy of 20 keV and a beam current of ca. 1 nA and typical magnification ca 5000 \times . This CC SEM-EDX is equipped with a Si(Li) detector that can work in windowless mode

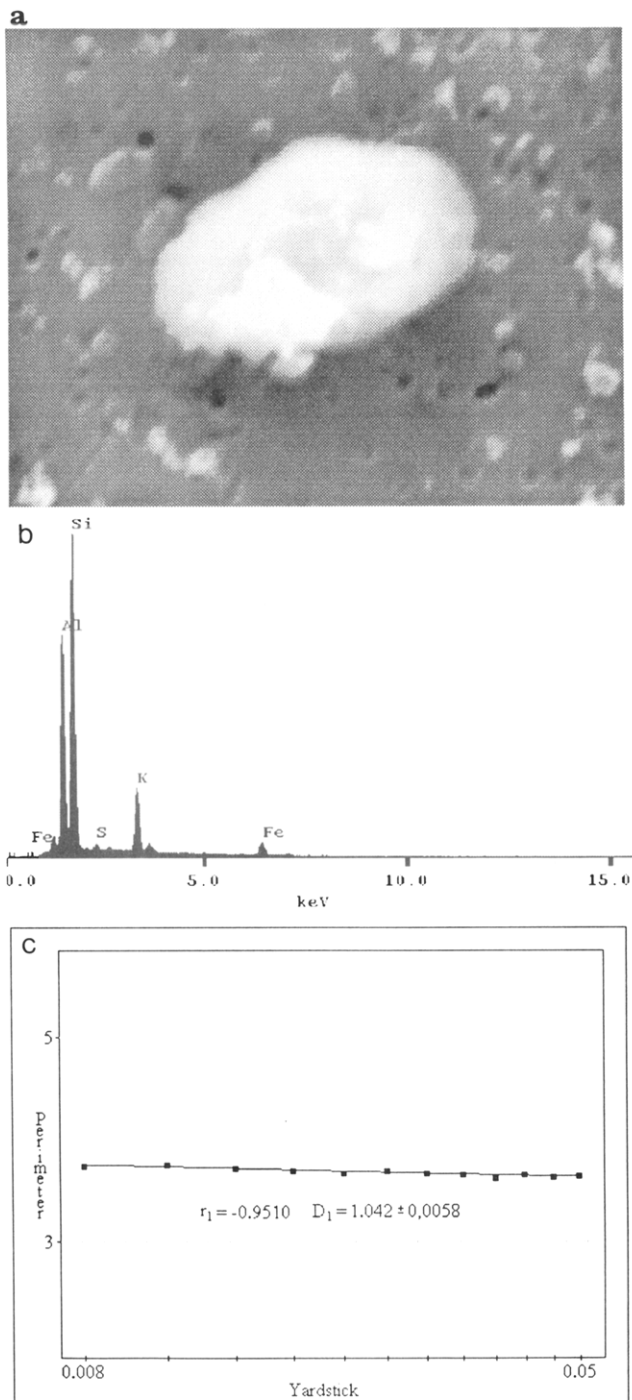


Figure 4. Soil dust particle: (a) SEM micrograph; (b) EDX spectrum; (c) fractal analysis.

(PGT-IMIX). The IMIX (Integrated Microscope and X-ray microanalyzer) provides powerful image acquisition and processing possibilities. Details of the image processing technique used are described in the Appendix.

Results and Discussion

A typical example of a spherical fly ash particle, its EDX spectrum, and the results of the fractal analysis are presented in Figure 2a-c. The first three points in Figure 2c demonstrate a type of "dependence" that can be attributed to the digital nature of the image (fractal rabbit, see above). The coefficient of correlation seems reliable, the fractal dimension differs statistically significantly from unity. The second straight line obviously demonstrates

Table 1. Fractional Diameters ± Standard Deviations for Three Different Types of Individual Aerosol Particles

type of aerosol particle	no. of particles under study	fractal dimension	
		textural	structural
spherically shaped fly ash	35	no	no
irregularly shaped fly ash	21	1.09 ± 0.015	1.28 ± 0.020
soil dust	37	1.04 ± 0.013	no

the absence of fractality for this spherically shaped fly ash particle. So, we can conclude that spherically shaped particles do not possess fractality.

A picture of a fly ash particle with very irregular shape, its EDX spectrum, and the results of fractal analysis are given in Figure 3a-c. The differences in the composition as well as the differences in shape compared to the previously studied fly ash particle are explained by the different origin. Consequently, the results of the fractal analysis are also different. Two different dependencies are seen in Figure 3c, corresponding to two different fractal dimensions. It is interesting to note that there are no fractal rabbits in Figure 3c. Summarizing, we can state that irregularly shaped fly ash particles possess two-mode fractal dimensions with significant statistical differences between the dimensions.

A micrograph of a soil dust particle, its EDX spectrum, and the results of fractal analysis are shown in Figure 4a-c. Comparison of Figures 2a and 4a leads to the conclusion that it is impossible to judge about the belonging of the particle to the fly ash or soil dust classes solely on the base of the composition. At the same time, fractal analysis reveals interesting things. The first three points form a fractal rabbit, just as it was in the case of spherically shaped fly ash particle. At the same time, textural fractality is evident from Figure 4c. The yardsticks larger than 0.05 of Feret diameter do not possess any kind of dependence, indicating the absence of a structural fractality.

The results of studying these three types of individual aerosol particles are summarized in Table 1. The absolute values of the fractal dimensions of the particles of the same class vary significantly. However, the phenomena of the absence of fractality for the spherically shaped fly ash particles, the presence of both textural and structural fractality for the irregularly shaped fly ash particles, and the presence of only textural fractality for soil dust particles hold for all the particles under analysis.

After this paper had already been prepared, an article by Xie et al. (16) dealing with nearly the same subject appeared. The results of the calculations of fractal dimensions nearly coincide. However, the authors of the paper (16) did not pay attention to the possibility of fractal rabbits when determining the fractal dimension of the spherically shaped particles. Therefore, their results for this type of particles are not completely correct. Unfortunately, they also did not specify the accuracy of the determination of the fractal dimensions, so it can be hardy judged if airborne particles of different nature can be distinguished according to their fractal dimensions.

Still, the appearance of the paper (16) along with the present paper indicates that the fractal approach becomes a practical tool in the analysis of individual aerosol particles.

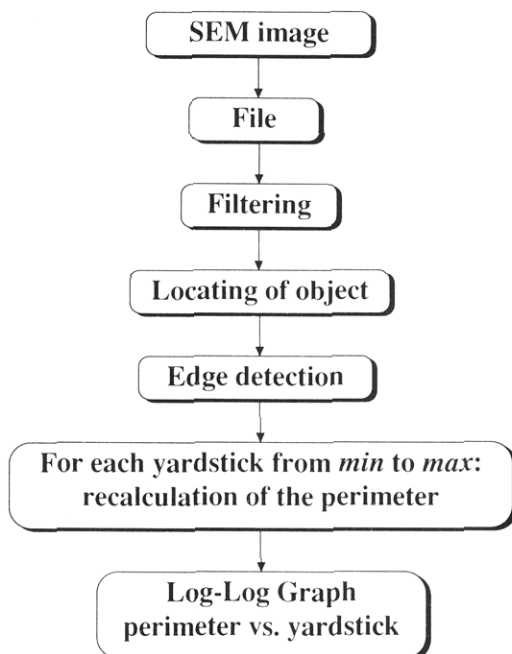


Figure 5. Flow chart of the SEM image processing.

Conclusions

The results of the fractal analysis of the SEM images of the two main types of fly ash particles (spherically shaped and with irregular forms) show that they have a different fractal behavior. Spherically shaped particles have no fractality at all, whereas irregularly shaped particles are characterized by both textural and structural fractal dimensions. Soil dust particles, in their turn, can be characterized only by textural fractal dimension. The regularities found can be used for the unequivocal differentiation between soil dust and fly ash particles, thus allowing correct particle source apportionment.

Acknowledgments

This study was partially supported by the Belgian NFWO. We are grateful to H. Van Malderen (University of Antwerp, Belgium) and K. P. Kutsenogii (Institute of Chemical Kinetics and Combustion, Russian Academy of Sciences, Novosibirsk, Russia) for collecting the samples.

Appendix

Image Processing. The flow chart of the SEM image processing is given in Figure 5. The images are processed off-line on PC AT with the help of in-house-developed Windows based software.

Median filtering was used to decrease the noise and increase the signal/background ratio of the images. Then the initial 256 gray-scale level images were converted into binary ones.

In order to locate the particle in the image, we found at first if only one point was inside the particle. This procedure is illustrated in Figure 6. The point is considered as lying inside the particle if all points that surround it in all eight directions within the step d belong to the particle or its border. The next problem is to detect the edges (contour) of the particle. The algorithm (see Figure 7) is similar to that described in ref 17. It starts from the point A, determined in the previous step, and proceeds directly down until a point that does not belong to the particle (by the above given definition) is reached (here, point 0). Then

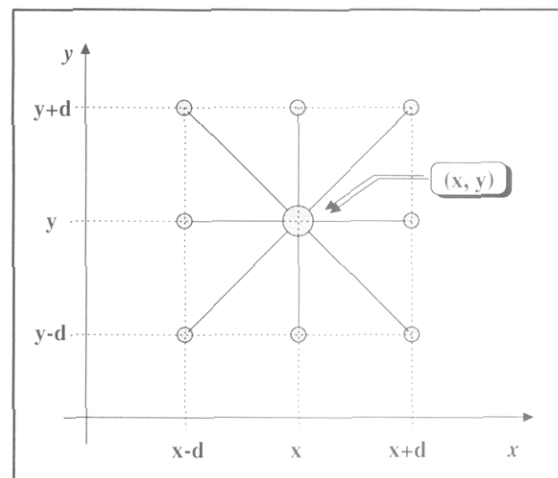


Figure 6. Illustration of the definition of the point, which lies inside the particle.

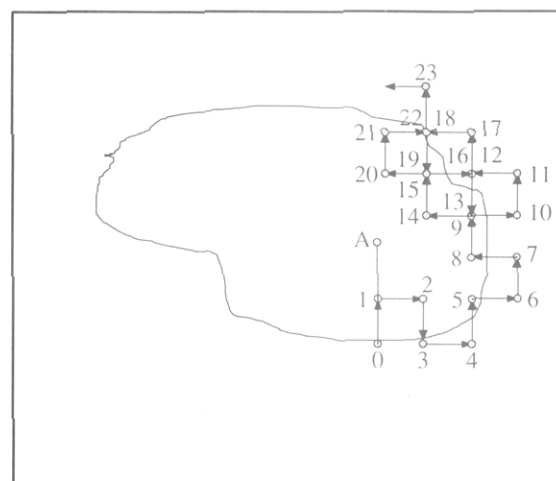


Figure 7. Explanation of the algorithm for the detection of the particle image contour.

Table 2. Values of Feret Diameters, Coefficients of Correlation of Linear Regression Straight Lines, Fractal Dimensions, and Their RMS Errors for Different Thresholds of Image from Figure 4a

no.	threshold	Feret diameter	coefficient of correlation	fractal dimension	error
1	100	285.5	-0.96	1.039	±0.0071
2	105	284.0	-0.97	1.040	±0.0062
3	110	282.1	-0.94	1.037	±0.0080
4	115	279.4	-0.97	1.045	±0.0071
5	120	278.7	-0.89	1.031	±0.0097
6	125	276.7	-0.91	1.034	±0.0094
7	130	276.0	-0.94	1.042	±0.0093
8	135	274.3	-0.96	1.047	±0.0074
9	140	273.2	-0.95	1.044	±0.0081
10	145	271.4	-0.91	1.036	±0.0096
11	150	267.0	-0.96	1.049	±0.0084
12	160	267.2	-0.95	1.042	±0.0085
13	170	264.2	-0.96	1.039	±0.0066
14	180	256.6	-0.96	1.035	±0.0059
15	190	249.0	-0.98	1.047	±0.0052
16	200	244.4	-0.97	1.056	±0.0085

it goes one step back to point 1 and turns all the time to the right if the point is inside the contour of the particle or to the left otherwise. Once the contour is detected, its Feret diameter is calculated.

The next step of the algorithm is the measuring of the perimeter of the particle with different yardsticks (in

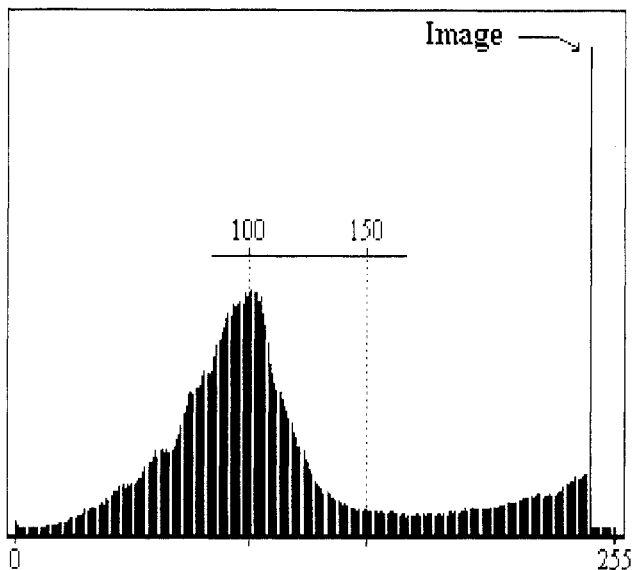


Figure 8. Histogram of brightness of the image shown in Figure 4a.

fractions of the Feret diameter), starting normally from the $min = 0.01$ to $max = 0.2$. The calculation of the perimeter is based on the method proposed in ref 5, which is faster than exact hand and dividers method and is more accurate than the often-used fast algorithm by Schwarz and Exner (18).

The last step of image processing is the drawing of Richardson plots for the determination of the fractal dimensions D from the slopes of the correspondent linear regression straight lines as was described in the Brief Overview section. The root mean square error of the regression line is calculated, allowing us to calculate the unbiased estimates of the standard deviations for the correspondent values.

It is important to emphasize that this procedure is practically independent on the choice of the threshold when converting a 256 gray-scale image into a binary one. This fact is illustrated in Table 2 where fractal dimensions and their root mean square (RMS) errors for 16 different thresholds of the image presented in Figure 4a are given. The correspondent histogram of brightness is shown in

Figure 8. The conditions for fractal analysis are the same in the case of fractal analysis in Figure 4c. It is seen that in spite of the slight variation of the absolute value of the fractal dimension, a soil dust particle possess a textural fractal dimension.

Literature Cited

- (1) Xie, Y.; Hopke, P. K. *Abstracts; American Association of Aerosol Research, 12th Annual Meeting, Oak Brook, IL, Oct 11-15, 1993*; p 198.
- (2) Raeymaekers, B.; Van Espen, P.; Adams, F. *Mikrochim. Acta* 1984, 2, 437-454.
- (3) Duda, R. O.; Hart, P. E. *Pattern Classification and Scene Analysis*; Wiley: New York, 1973; Chapter 9.
- (4) Medalia, A. I. *Powder Technol.* 1970/71, 4, 117-138.
- (5) Clark, N. N. *Powder Technol.* 1986, 46, 45-52.
- (6) Normand, M. D.; Peleg, M. *Powder Technol.* 1986, 45, 271-275.
- (7) Hopke, P. K.; Casuccio, G. S.; Mershon, W. J.; Lee, R. J. *Scientific Computing and Automation (Europe)*; Elsevier: Amsterdam, 1990; pp 173-178.
- (8) Cheng, S. H.; Lin, J. C.; Wu, J.-R.; Gentry, J. W. *J. Aerosol Sci.* 1994, 25 (Suppl. 1), S379-S380.
- (9) Kaye, B. H. *A Random Walk Through Fractal Dimensions*; VCH: Weinheim, 1989.
- (10) Mandelbrot, B. B. *The Fractal Geometry of Nature*; Freeman: New York, 1983.
- (11) Orford, J. D.; Whalley, W. B. *Sedimentology* 1983, 30, 655-668.
- (12) Julian, K.; Mills, S. L. *Anal. Proc.* 1993, 30, 229-232.
- (13) Lerche, L. *PAGEOPH* 1993, 140, 503-517.
- (14) Fisher, J. E.; Prentice, B. A.; Silberman, D.; Ondov, J. M.; Biermann, A. H.; Ragaini, R. C.; McFarland, A. R. *Environ. Sci. Technol.* 1978, 12, 447-451.
- (15) Ramsden, A. R.; Shiraoka, M. *Atmos. Environ.* 1982, 16, 2191-2206.
- (16) Xie, Y.; Hopke, P. K.; Casuccio, G.; Henderson, B. *Aerosol Sci. Technol.* 1994, 20, 161-168.
- (17) Jain, A. K. *Fundamentals of Digital Image Processing*; Prentice-Hall: Englewood Cliffs, NJ, 1989; Chapter 9.
- (18) Schwarz, H.; Exner, H. E. *Powder Technol.* 1980, 27, 207-213.

Received for review March 30, 1994. Revised manuscript received August 8, 1994. Accepted August 11, 1994.*

* Abstract published in *Advance ACS Abstracts*, September 15, 1994.